PERGAMON

Microelectronics Reliability 40 (2000) 981–990

MICROELECTRONICS RELIABILITY

www.elsevier.com/locate/microrel

The evolution of the resistance of aluminum interconnects during electromigration

Jonathan C. Doan [a,*], John C. Bravman [a], Paul A. Flinn [a], Thomas N. Marieb [b]

[a] *Department of Materials Science and Engineering, Stanford University, 416 Escondio Mall, Stanford, CA 94305-2205, USA*
[b] *Components Research, Intel Corporation, 3065 Bowers Avenue, Santa Clara, CA 95052-8119, USA*

Received 12 October 1999; received in revised form 16 December 1999

Abstract

Resistance monitoring is a traditional method to investigate electromigration failure. It is important to understand how much information can be extracted from the data generated by these experiments. To this end, precision resistance measurements were included as part of accelerated electromigration tests performed inside of a high voltage scanning electron microscope (HVSEM). Twenty-two passivated Al interconnects were tested at 30 mA/μm^2 and at two temperatures, half at 212°C and half at 269°C. During every test, our automated apparatus stored images of each 300 μm long structure several times per hour. The resistance of each line was also precisely measured and recorded. Changing the temperature affected only the time scale of the resistance evolution. There were resistance changes before voids formed that were neither due to temperature fluctuations nor solute effects. In most cases, the nucleation of the first void to form in a line was signaled by an increase in the time derivative of the resistance. Due to the strong effect of void shape, the void volume could not be determined by the magnitude of the resistance change. The width of a void (transverse to the line) rather than the volume largely determined the resistance change.

1. Introduction

The resistance change in interconnects has long been used to study electromigration damage [1–7]. From a research standpoint, it would be useful if the resistance data could be interpreted in terms of the stages of the failure progression. Electromigration failure is a dynamic process consisting of void nucleation, growth, motion, and shape evolution [8–12]. Qualitative interpretations of the resistance data could be used to understand how a certain set of specimens fail. Quantitative relations between resistance data and void behavior could be used to validate models. The extraction of void nucleation times, growth rates, and dynamic behavior would be beneficial. In this article, we will use simultaneous observation of voiding and measurement of resistance to determine how much information can be learned from the resistance data alone.

1.1. Background

In 1968, Rosenberg and Berenbaum were among the first researchers to study electromigration with a resistance measurement technique [1]. Lloyd and Koch introduced the use of an AC Wheatstone-bridge circuit to measure more accurately the resistance of a test line [3]. Additionally, they reintroduced a hypothesis of Bobbio and Saracco [13] in which the initial rate of resistance increase might correlate inversely with the lifetime of a sample. Maiz and Segura found that this hypothesis was true for the average rate of resistance change and the median time to failure (MTTF) of a population of lines [4]. A measurement of the initial slope of the resistance versus time curve can be made rather quickly. If this slope always correlated with the MTTF of a set of lines, precise resistance measurements would be a potentially fast method to determine interconnect reliability. The

* Corresponding author.
E-mail address: jondo@stanford.edu (J.C. Doan).

0026-2714/00/$ - see front matter
PII: S0026-2714(99)00340-6

results of these early experiments have motivated a substantial amount of research in this area [14–18].

In situ techniques have often been used to shed light on electromigration mechanisms. Two groups have correlated observations from electromigration tests in situ in a scanning electron microscope (SEM) with measurements of the line resistance [19,20]. Both of these reports suffered from the problem of imaging only a small portion of the entire test structure. The work performed by Shingubara et al. focused primarily on abrupt changes in resistance of a very small magnitude and found that these events often occurred during void motion [19].

Li et al. simultaneously measured void area and line resistance during accelerated tests in a SEM [20]. Plots of the fractional resistance change versus time and the fractional voided area versus time were qualitatively similar. Due to this resemblance, they proposed that the fractional resistance change was proportional to the void volume (the voids were assumed to extend through the thickness of the line with vertical walls). The resistance measurement probed the entire line for electromigration damage, while the SEM observation focused on only a small area. The restricted area under visual study may have complicated their findings.

In a closely related (although not in-situ) study, Miner et al. examined void sizes at failure ($\Delta R/R = 20\%$) in via-line structures [21]. They used a transmission electron microscope (TEM) and a SEM to measure the voids. In their experiments, the sizes of the voids (located at the cathode vias) scaled with the lifetime of each line. This implied that the voids grew roughly linearly with time. The size of the void required to cause the 20% resistance increase varied greatly from line to line. They proposed that the resistance change depended critically on the shape of the void and the resultant path of current flow around the void. These results suggest that the resistance change is not simply proportional to void volume. In this article, we examine this relationship in detail.

2. Experimental

2.1. Specimen preparation

Six-inch Si wafers were oxidized to form 55 nm of SiO_2. After oxidation, 25 nm of Ti, 720 nm of Al, and 5 nm of TiN were deposited on the wafers. Structures were patterned using standard photolithographic techniques and the wafers were etched and cleaned. A protective 100 nm layer of PECVD SiO_2 was deposited onto the test structures. At this point, the specimens were annealed at 400°C for five hours. The Ti reacted with the Al to form $TiAl_3$ during this annealing step. After the reaction, there were approximately 650 nm of Al and 90 nm of $TiAl_3$. A 1 μm final passivation of (PTEOS) SiO_2 was deposited at 400°C. Finally, all of the samples were annealed again for 11 h at 390°C to ensure a complete reaction of the Ti with the Al and to completely stabilize the Al microstructure. The test structures were 300 μm long and 2.6 μm wide.

2.2. Resistance measurement

In many applications, the precision of a resistance measurement is limited by temperature fluctuations. In our experiments, this problem is exacerbated by testing in vacuum. Due to the limited paths for heat flow, large temperature gradients can develop. To minimize this, the heating stage on our apparatus was constructed to be small, thermally conductive, and well insulated from its surroundings. A platinum resistance thermometer mounted next to the specimen measured the temperature of the stage. With an active feedback system, the stage temperature was constant to within 0.1 K over the duration of a test (up to several hundred hours).

Due to the vacuum environment, the temperature of the test structure differed slightly from that of the resistance thermometer. To measure and compensate for this effect, the resistances of the lines were calibrated as a function of temperature. For this task, an oven was specially constructed to be thermally uniform. In this way, each line could serve as its own thermometer to set the test temperature. It was assumed that the temperature difference between the line and the heating stage remained constant during a test. Monitoring the resistance of a neighboring line validated this assumption.

Microstructural changes unassociated with electromigration can induce resistance changes in a test line. As discussed in the previous section, the specimens were thoroughly annealed, twice, during processing. Each of these annealing steps was sufficient to form a stable microstructure. Finally, before the start of each test, the sample die was held at the test temperature for 10–12 h. If microstructural changes unrelated to electromigration were to occur, they would affect the resistance of the monitor line. Since no such effects were measured, we concluded that these specimens had a stable microstructure at the start of each test.

The thermoelectric effect can confuse measurements of resistance at high temperature. We periodically check for errors in the measurement of the line voltage due to this effect, but it was never detected. Electrical noise can also reduce the precision of resistance measurements, so custom circuitry was constructed to minimize this problem. The circuitry suffered from background noise of roughly two-tenths of a millivolt. This level was considered acceptable, as the relative resistance change was precise to 0.04% for lines under testing.

2.3. In situ testing with high voltage SEM

We employed backscattered-electron imaging to view lines under passivation layers. High-energy (120 keV) electrons penetrated through thick (>1 μm) passivation layers, elastically scattered from the metal line and escaped back through the passivation. A reversed-biased p-n junction counted the reflected electrons. The magnitude of the backscattered electron current from each point on the specimen was mapped to form an image. This technique has been shown to provide relatively high resolution (50 nm) through thick (0.5 μm) dielectric layers [22].

The scan ratio of the HVSEM was modified to image an entire 300 μm long line at a reasonable magnification. One such image is shown in Fig. 1. In these images, aluminum appears light gray, while voids and silicon appear black. The capability of the HVSEM to image an entire line was critical to this project. Voids that formed in any section of a line were immediately detected. With this information, the resistance changes could be compared to the void behavior. The HVSEM apparatus is discussed in more detail elsewhere [23].

Two groups of 11 specimens were tested at two different temperatures. One group of samples was tested at 212°C, while the other group was tested at 269°C. The test temperatures include approximately 7°C of Joule heating. The current density for every test was 30 mA/μm^2. The failure criterion was a resistance increase of 30%. Every test was run inside of the HVSEM, where a digital image was collected and stored every 4 ($T = 269$°C) or 8 ($T = 212$°C) min. After each test was completed, an automated image-recognition algorithm determined the positions and sizes of the voids in every image.

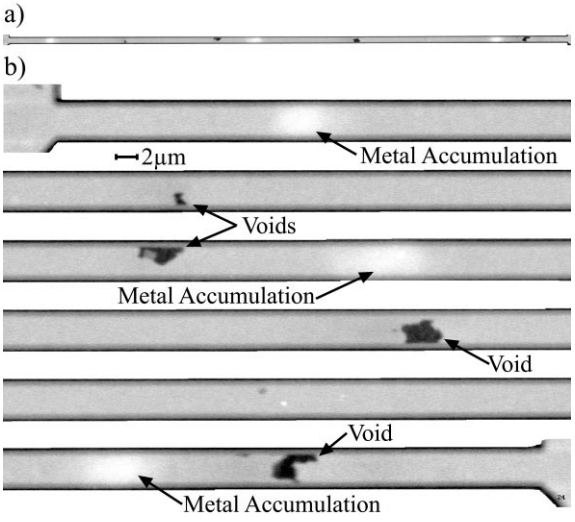

Fig. 1. (a) A 50:1 HVSEM image of an aluminum test line during an electromigration test. The image is 300 μm long. (b) The same 300 μm image cut into six sections and displayed at a higher magnification.

3. Data and results

The evolution of the resistance can be classified into three stages in our experiments. Initially, there were small resistance changes that were both positive and negative in sign. After a period of time, the resistance increased more rapidly and monotonically. After the resistance rose by approximately 5%, it rapidly increased to a 30% change and the tests were over. Occasionally, just as the line was apparently failing, the resistance would rapidly decrease and the lifetime would be extended.

This categorization can be seen in Fig. 2. During the experiment represented by the lower curve, the resistance first decreased slowly and smoothly with time. After 46 h (a), the first void in the line nucleated and the resistance began to rise. Approximately 10 h later (b), the resistance increased quickly to 30% and the test was over.

In the experiment marked by the upper curve in Fig. 2, the resistance first increased and then plateaued. After 20 h (1), a void nucleated and the resistance began to rise again. Approximately 32 h into the test (2), it appeared that the line would fail, due to a void that was about to sever the line. However, the void moved, changed shape and the life of the line was prolonged. Fifteen hours later (3), another void caused the failure of the interconnect.

3.1. Early resistance changes

There were measurable resistance changes in nearly every line before any voids nucleated. These early resistance changes were both positive and negative and ranged from +2% to −1%. The resistance changes before voids nucleated are shown for two lines in Fig. 3. In

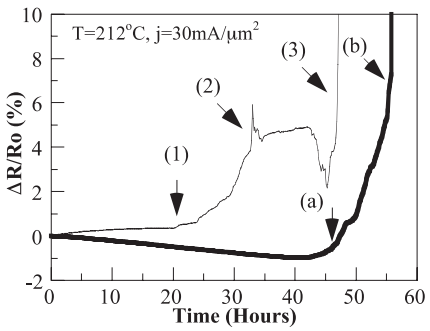

Fig. 2. The evolution of the resistance can be classified into three stages.

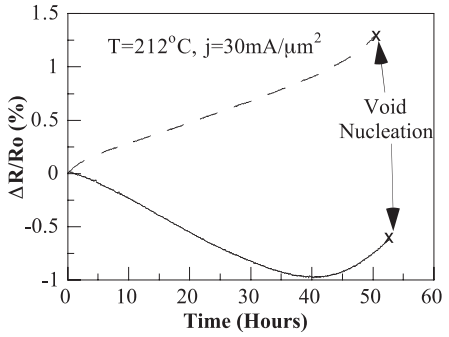

Fig. 3. The early resistance changes during two in situ experiments. The first voids nucleated 50.3 and 52.7 h into the tests.

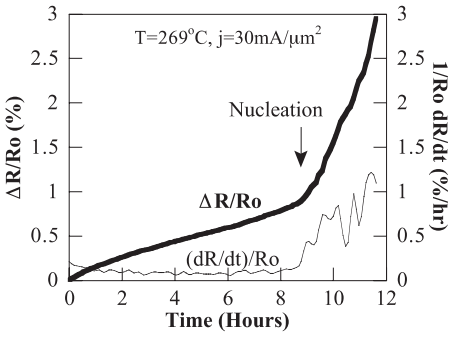

Fig. 5. The nucleation of the first void in a test is accompanied by a change in the slope of the resistance versus time plot.

these two experiments, the time to the nucleation of the first void was approximately the same. This was not true in general. It was important to determine if these resistance changes were induced by electromigration or some other effect.

Fluctuations in temperature would have affected the resistivity of the metal and might have accounted for the early resistance changes. To test for this, we monitored the resistance of a neighboring line. The resistance change of an interconnect under testing and the corresponding monitor line are plotted in Fig. 4. The resistance of the tested line increased by 1.3%, while the resistance of the monitor line remained constant. Temperature fluctuations of the specimen die did not cause the observed resistance changes.

3.2. Void nucleation

In theory, once a void nucleates, the resistance of the line should increase. However, it was not clear, at first, that the resistance changes from a small void would be detectable over the background of the early resistance changes. In fact, in 80% of the tests, the nucleation of the first void caused a measurable change in the slope of the resistance versus time curve. One example of this is shown in Fig. 5. The determination of the nucleation time for the first void in a test represents extra information one can extract from the resistance versus time data. The nucleation time was confirmed independently through direct observation in the HVSEM.

In four samples out of 22, the first void to nucleate could not be detected from the resistance data alone. The first void in each of these tests grew slowly at the start. The changes in resistance from the voids were indistinguishable from the "background" of the early resistance changes. Data from one such experiment are plotted in Fig. 6. The nucleation time of the first void would have been overestimated by 10–15%. In each case, the slope of the resistance versus time curve eventually increased either by the original void beginning to grow more quickly, or another void nucleating and growing. Due to the stochastic nature of nucleation times [24], these few overestimates would only slightly shift the distribution of nucleation times measured in this manner.

After the resistance increased due to void nucleation and growth, the nucleation of new voids could not be detected from the resistance data. The number of voids

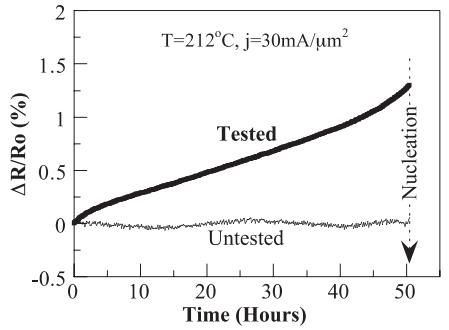

Fig. 4. An untested, monitor line shows no resistance change. The first void nucleated in the tested line just after 50 h of testing.

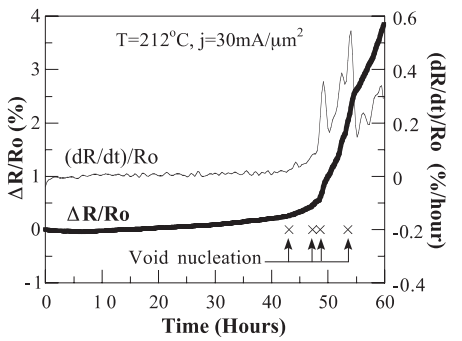

Fig. 6. In this experiment, the time derivative of the resistance did not increase until after the second void in the test nucleated.

in each line ranged from 1 to 11 at the end of the test. On average, there were four voids per line. Upon the background of the relatively small and smooth early resistance changes, a newly formed void generally produced a measurable shift. Once a void was large enough to affect the resistance significantly, the dynamic changes in the resistance due to this void obscured the small effects of any new nucleation events.

3.3. Void growth and resistance increase

To evaluate models of void growth, it would be useful to infer the void volume from the changes in resistance of a line. If one knew the shape, size and location of every void in an interconnect, the resistance change due to those voids could be calculated in a straightforward manner. The forward calculation is relatively easy; can one perform the reverse operation? In general, the answer to this question is "no." The resistance of a line is not a unique function of the void volume. This is shown in Fig. 7, where two line segments with voids of equal volume would have vastly different resistances. The resistance of a voided line depends on the shape of the voids.

One might hypothesize that in a given interconnect system, every void assumes a well-defined shape. If this were the case, then the resistance change due to a void could be uniquely related to its volume. Data from eight in situ experiments are plotted in Fig. 8. It is clear that the resistance change was not a unique function of the void volume. It is also apparent that the change in resistance was not a linear function of the void volume. Both the size and shape of a void determine its effect on the resistance.

The strong dependence of resistance on the shape of a void is shown in Figs. 9 and 10. In this test, the resistance increased by almost 30% for a negligible change in void volume. Only by a careful study of Fig. 10 can the reason for the resistance increase be found. There was a very small change in the shape of the tip of the void.

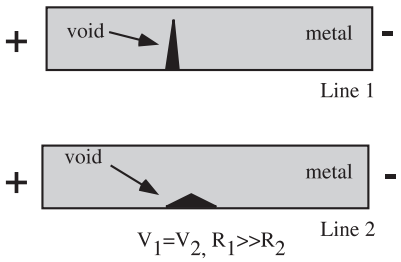

Fig. 7. The two interconnect segments have triangular voids of equal volume. However, segment 1 clearly has a much higher resistance.

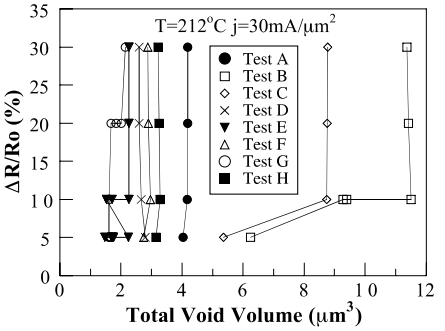

Fig. 8. The resistance change is not a unique function of void volume. These data are from eight in situ electromigration tests.

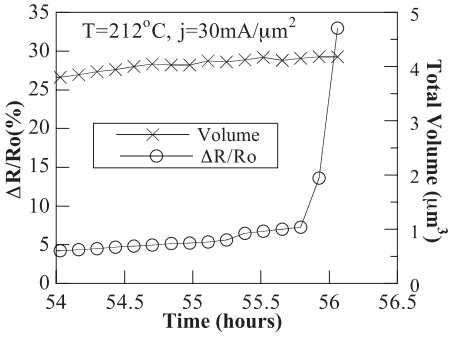

Fig. 9. The resistance changes substantially for a negligible change in the void volume.

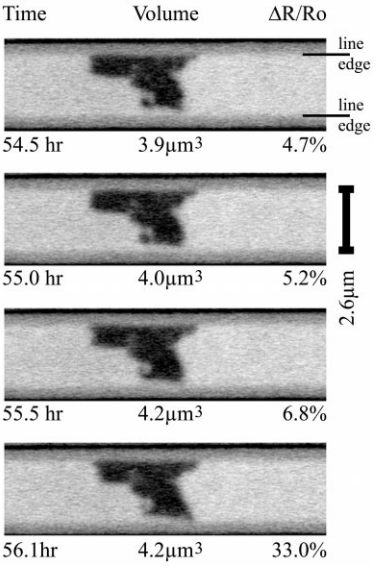

Fig. 10. A very small change in shape causes a large change in resistance. The images in this figure were selected from the experiment shown in Fig. 9.

This slight rearrangement was responsible for the 26% increase in resistance. There was one other void in this line. It was small and stable and could not have affected the resistance in any appreciable manner.

Fig. 10 demonstrates that large resistance changes can arise from very small changes in void shape. The morphology of a void was especially important when it extended across most of the line width. Perhaps when voids are much smaller, void shape would be less important. Assuming a rectangular void and a series resistor model, the resistance of a line is approximately,

$$R = \frac{\rho(L - L_v)}{wt} + \frac{\rho L_v}{(w - w_v)t}, \tag{1}$$

where ρ is the resistivity of the metal, L, w and t are the interconnect length, width and thickness, and L_v and w_v are the void's length and width. Using the Taylor expansion around $w_v = 0$, Eq. (1) becomes

$$\frac{\Delta R}{R_0} = \frac{V_v}{V}, \tag{2}$$

where, R_0 is the initial resistance of the line ($\rho L/wt$), V_v is the void volume and V is the volume of the line (Lwt). Eq. (2) is independent of the void shape.

The resistance change is plotted as a function of the void volume in Fig. 11 for very small voids. The data are from the eight tests that were shown in Fig. 8. Even for small voids, the fractional resistance changes were neither equal to, nor even a unique function of, the fractional void volume. If one had estimated the void volumes based on the resistance changes, the resulting values would have been incorrect by as much as a factor of five. Even for very small voids, one cannot infer volumes from the resistance changes.

Eq. (1) does not account for the alteration of the current flow in the neighborhood of the void. Because of this, Eqs. (1) and (2) should be taken as lower bounds on the actual resistance change for a given void volume. From this assumption, all of the data points in Fig. 11 should lie above the black line. The few that do not are from samples in which the resistance had been decreasing prior to the nucleation of the void.

An examination of Fig. 10 suggests that the resistance change induced by a void strongly depends on the width of that void. Eq. (1) can be rearranged to produce

$$\frac{\Delta R}{R_0} = \frac{V_v}{L(w - w_v)t}. \tag{3}$$

This equation captures the critical dependence of the resistance change on the void width. The predictions of Eq. (3) are tested in Fig. 12, while the predictions of Eq. (2) are tested in Fig. 13. The same three sets of data are evaluated in each plot. These three tests were chosen because only one void formed in each. The void volume combined with the void width were much better predictors of the resistance change than the void volume alone. Eq. (3) described the data especially well for resistance changes under 5%. The deviations of the data from Eq. (3) were not surprising given the deviations of the void shapes from the assumed rectangles.

In practice, we are interested in predicting the volume from the measured resistance, and not the other way around. One cannot uniquely calculate the void width and volume from the resistance using Eq. (3). A void shape could be assumed to reduce the number of unknowns on the right side of Eq. (3) to one. Unfortunately, the shapes of voids changed substantially throughout the experiments. From void to void and test to test, the variations were even larger. Shape evolution

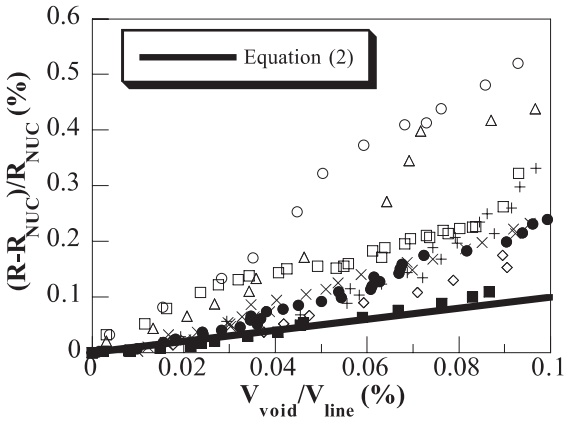

Fig. 11. Even for very small voids, the resistance is not proportional to void volume. Note that the resistance changes are relative to the resistance of the line at the time of nucleation.

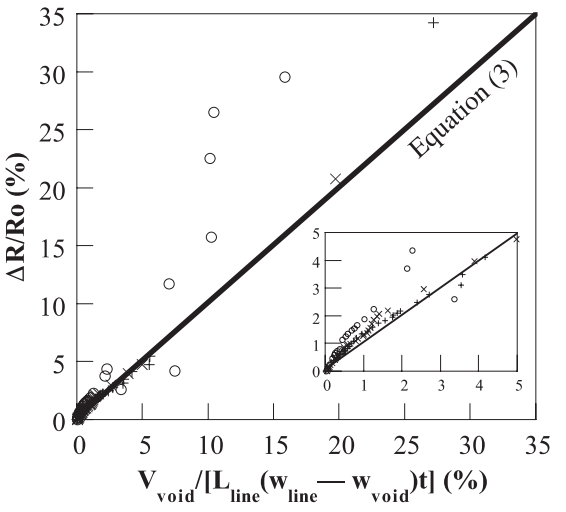

Fig. 12. In this plot, the effect of void shape is captured by independently measuring the void volume and width. The diagonal line represents the prediction of Eq. (3).

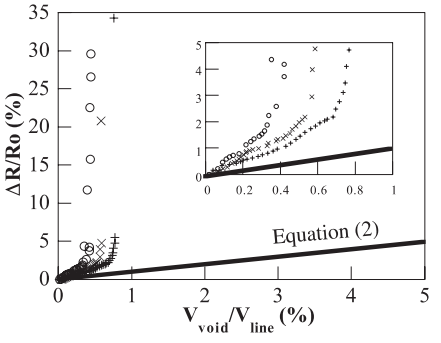

Fig. 13. In this plot, the resistance data from Fig. 12 are plotted against the fractional void volume. The diagonal line represents the predictions of Eq. (2).

of voids has been discussed elsewhere [25,26]. Because of this, it was not possible to predict void volumes from the measured resistance changes.

4. Discussion

4.1. The effect of test temperature

The resistance data from the high and low temperature tests were qualitatively similar. As one would expect, the time scale of the tests at 269°C was much shorter than that of the tests at 212°C. The examples given in the figures of this article were chosen to be a representative sample of the data from two different test conditions.

Of the four first voids that were not detectable from the resistance change alone, three were from the tests at the higher temperature. However, this is not a statistically significant difference. At this point, there would be no reason to suspect that such a systematic difference existed.

4.2. The early resistance change

Because the resolution limit of the HVSEM is 50 nm, one might suppose that there could be undetectable voids that affect the resistance of the line. Mechanical modeling of void nucleation suggests that once a stable void nucleus forms, it should very quickly grow to a resolvable size. Due to the energy barrier to form a stable void nucleus [27,28], large tensile stresses must develop before a void can form. Immediately after nucleation, these large stresses provide the driving force for rapid void growth. Once the local (within a radius roughly equal to half the line's thickness) stresses are relieved, further void growth depends on long-range mass transport that is relatively slower. This process is described in more detail elsewhere [24]. Additionally, studies using a TEM have never observed voids that were not visible in the HVSEM as well [29]. Because of the mechanical modeling and the TEM corroboration, we feel confident that once a void nucleates, it rapidly grows large enough to resolve in the HVSEM.

Many researchers have observed small early resistance changes [5,7,16,30]. Typically the explanations for this effect center on changes in the resistivity of the metal. Changes in vacancy and point defect concentrations, as well as piezoresistivity, have been proposed to explain this phenomenon.

Recently, De Ceuninck et al. have shown that, in many cases, early resistance changes are due to Cu atoms going in and out of solution [31]. Because our samples are pure Al, this effect cannot explain our observations. De Ceuninck also showed that the resistance of Al lines can change during the first annealing cycle. Since our specimens have been thoroughly annealed with a well controlled thermal history this cannot explain our observations either.

Because the Al lines have a $TiAl_3$ underlayer, it is possible that Ti atoms were going in and out of solution. However, the observed early resistance changes could not have been due to solute motion from the overall thermal cycling. If it were, the monitor line in Fig. 4 would have shown the same initial resistance increase as the tested line. If solute motion were responsible, the initial resistance change should have always been in the same direction because of the identical thermal cycling of every line.

De Ceuninck also showed that the Joule heating of a line during a test could be enough to cause a detectable resistance change. This was again due to Cu solute atoms going into solution at the slightly higher temperature. Using the resistivity change as a function of Ti concentration [32] and the solubility of Ti in Al [33], one can calculate that the Joule heating would need to be roughly 65 K to produce a 1% resistance increase. This is an order of magnitude higher than what was actually present (7 K). Additionally, this effect would only explain a resistance increase. The true mechanism must be able to explain both an increasing and decreasing resistance at the start of a test. From these considerations, we conclude that the early resistance changes are real and associated with electromigration.

The work of Kraayeveld et al. supports the finding of an early resistance change due to electromigration [16]. In their work on short Al lines, they found that the initial resistance change was positive or negative, depending on the direction of current flow. They also found that, if the current were high enough, the resistance would eventually begin to increase linearly with time. These observations seem similar to ours – an initial small resistance change of either sign followed later by a monotonic resistance increase.

Piezoresistivity coupled with the stress evolution during electromigration has been suggested as a possible

mechanism for resistance changes in interconnects [34,35]. As previously noted by Reilly and Sanchez [36], the resistance change due to piezoresistivity depends only on the change in the average hydrostatic stress in the line. To a reasonable approximation, the average hydrostatic stress does not change. Using Reilly's value of the piezoresistivity of Al ($d\rho/d\varepsilon_v = 2.0 \times 10^{-5}$ Ω cm) [36], one can calculate that the hydrostatic stress averaged over the length of the line would have to change by over 140 MPa to produce a resistance change of 1%. While the average stress could shift slightly, 140 MPa is an unrealistically high value. Thus, piezoresistivity cannot account for the early resistance changes we observe in our experiments.

Other authors have suggested that a change in the vacancy concentration is responsible for the early resistance change [37,38]. If one assumes that vacancies are in thermodynamic equilibrium, then the concentration of vacancies is given by

$$C = C_0 \exp\left(\frac{\sigma\Omega}{kT}\right), \tag{4}$$

where C_0 is the vacancy concentration in the presence of no stress, σ is the normal traction on the interface which is the vacancy source/sink, Ω is the atomic volume, k is Boltzmann's constant, and T is the temperature. Because Eq. (4) is nonlinear, the total number of vacancies can change, even for a perfectly antisymmetric stress profile. However, the decrease in the defect concentration on the compressive end of a diffusion path will compensate for the increase at the tensile end.

If we assume that vacancies are in equilibrium with the stress, then we can derive an analytic expression for the maximum resistance change due to a change in the vacancy concentration. For a given current density and path length, the greatest resistance change will occur when the steady-state stress profile [39] is reached

$$\sigma(x) = -\sigma_{\max}\frac{x}{l}, \quad -l \leqslant x \leqslant l, \tag{5}$$

where $\sigma_{\max}$ is the stress at the cathode end ($x = -l$). By combining Eqs. (4) and (5), using the resistivity change per vacancy fraction, $d\rho/d\chi$, and integrating the resistivity along the path length, the resistance change can be calculated to be

$$\frac{\Delta R}{R_0} = \frac{1}{\rho}\frac{d\rho}{d\chi}\exp\left(\frac{-E_v}{kT}\right) \times \left(\left(\sinh\left(\frac{\sigma_{\max}\Omega}{kT}\right)\Big/\left(\frac{\sigma_{\max}\Omega}{kT}\right)\right) - 1\right) \tag{6}$$

where ρ is the resistivity of the metal, and E_v is the activation energy for vacancy formation. Using $\rho =$ 5 μΩ cm [32], $d\rho/d\chi = 3$ μΩ cm/at.% [40], $E_v = 0.75$ eV [40], $\Omega = 1.66 \times 10^{-29}$ m^3 [41], and $T = 239$°C, one calculates that a stress of 7 GPa is required at the cathode end of the path for a 1% resistance change. This unrealistically high [28] value of stress suggests that another mechanism might be responsible. Once again, this effect could explain resistance increases, but not decreases.

An alternative hypothesis to a resistivity change is that the grain boundary network of the thin film is changing. Mass transport due to electromigration could change the structure of the grain boundaries. The resistance of an Al grain boundary transverse to a line is on the order of 10^{-15} Ω m^2 [42]. Assuming that the line is composed of an array of square grains of the median grain diameter (0.8 μm), the grain boundaries contribute roughly 5% of the total resistance in a line. From this value, it seems possible that the −1–2% early resistance changes could have been due to changes in the grain boundary structure.

4.3. Extrapolation of the rate of resistance change

In the experiments of Maiz and Segura, the average resistance increased linearly with time from the beginning of the test [4]. They attributed the increase in resistance to the growth of many small voids. The presence of the voids was verified by visual observations. The initial resistance changes in these interconnects were due to the growth of voids. The resistance increased more quickly for lines in which voids grew more quickly. Lines in which voids grew quickly failed sooner. This picture has intuitive appeal.

In our specimens, there is a long period before the formation of voids. During this time, the resistance changes measurably. In the experiments of Maiz and Segura, the initial resistance changes were caused by void growth – the destructive process responsible for line failure. In our experiments, the early resistance changes were due to some other mechanism. It is not clear whether this early resistance changes due to this other mechanism should correlate with failure times. This seems especially true when one considers that the initial resistance changes in our structures are both positive and negative.

Maiz and Segura showed that the average rate of resistance change due to void growth was inversely proportional to the median time to failure of a population of lines. The resistance changes due to voiding just happened to occur at the very beginning of their tests. Because the nucleation of voids can be detected from the resistance data, in principle, one could measure the rate of resistance change after voids nucleated. At that point, the resistance change would be dominated by the growth of voids. One might expect to recover the results of Maiz and Segura in this way. Unfortunately, this method would sacrifice the most desirable feature of the resistance extrapolation procedure, speed. Nucleation times can be a substantial fraction of a line's lifetime [24]. In such structures, predicting lifetimes by extrapolating the

resistance change after nucleation would not be dramatically shorter than simply measuring the lifetimes outright.

Shih and Greer investigated the distribution of damage sites in unpassivated Al-4%Cu lines [43]. They observed a linear increase in damage sites with time and a linear relation between the number of damage sites and the relative resistance change. Additionally, the damage rates scaled inversely with the lifetimes. These observations are similar to those of Maiz and Segura. These findings are not surprising due to the fact that they studied unpassivated specimens. The presence of passivation quantitatively and qualitatively affects electromigration failure [9,44–46]. The dielectric layer plays two key roles. First, it constrains the line and changes the evolution of the stress. Second, it protects the surface of the metal. Damaged or contaminated areas of the surface could serve as nucleation sites. The fact that their damage rate was constant with time implies that the barrier for void nucleation was low (i.e. voids began to from at the beginning of each test). One would expect to observe the behavior described by Maiz and Segura in specimens with a low nucleation barrier.

In another series of experiments, we eliminated the nucleation barrier by implanting Al lines with Ar ions [47]. This produced many small bubbles that served as nucleation sites. Many small voids grew immediately from the onset of the accelerated test. In these experiments, the resistance increased roughly linearly with time until voids grew to sizes comparable to the line width. A plot of the resistance versus time for one of these tests is shown in Fig. 14. One can imagine that, in these specimens, the early rate of resistance change might be inversely proportional to failure times, as in the experiments of Maiz and Segura. However, in specimens with a substantial nucleation barrier, the early changes in resistance are not due to the process that causes line failure.

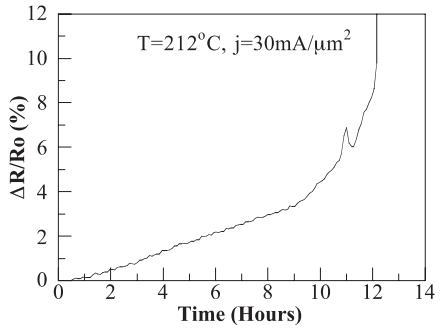

Fig. 14. Specimens with no nucleation barrier showed an initially linear resistance increase.

5. Conclusions

In most cases, the time at which the first void nucleated in a line could be found from the resistance measurement alone. Voids that nucleated subsequently could not be detected in the same manner. Our lines were relatively short, which helped the early detection of voids. The relative resistance change in a longer line would have been smaller. In such a structure, it would be more difficult to detect nucleation above the background changes. Due to the strong dependence of resistance on void shape, the total void volume could not be determined from the magnitude of the resistance changes. Aside from the distribution of void nucleation times, the extraction of quantitative details about the voiding process appears unwarranted.

In our experiments, the period before voids formed was a substantial fraction of the lines' lifetimes. Due to the resistance changes during this time, it is not clear whether the initial rate of resistance increase can be extrapolated to predict failure times. The mechanism responsible for the initial resistance increase in the experiments of Maiz and Segura was known to be the growth of voids from the start of the test. In contrast, the mechanism for the early resistance change in our specimens is unknown, and the initial rate of resistance change is unlikely to relate in any simple way to the failure of a line. We hypothesize that this is true for any sample set with long nucleation times.

We feel it is plausible that the early resistance changes are tied to a restructuring of the grain boundary network. Stress generation due to electromigration necessarily depends on the creation and annihilation of vacancies. To create vacancies, a structural change, such as dislocation climb, must occur. High-resolution resistance measurements could be used to investigate the early resistance changes during electromigration. An understanding of these basic processes would benefit efforts to improve interconnect reliability.

Acknowledgements

We gratefully acknowledge Components Research of Intel Corporation for the use of the HVSEM. One author (J.C.D.) would like to thank the Semiconductor Research Corporation for support in the form of a graduate research fellowship. We also acknowledge the support of the SIA Focused Research Center on Interconnects.

References

[1] Rosenberg R, Berenbaum L. Appl Phys Lett 1968;12:201.
[2] Hummel RE, Dehoff RT, Geier HJ. J Phys Chem Solids 1976;37:73.

[3] Lloyd JR, Koch RH. Appl Phys Lett 1988;52:194.
[4] Maiz JA, Segura I. Proc 26th IEEE IRPS 1988. p. 209.
[5] Scorzoni A, Cardinali GC, Baldini GL, Soncini G. Microelectron Reliab 1990;30:123.
[6] Niehof J, Flinn PA, Maloney TJ. Qual Reliab Eng Int 1993;9:295.
[7] Mockl UE, Lloyd JR, Arzt E. Mat Res Soc Symp Proc 1993;309:301.
[8] Blech IA, Meieran ES. J Appl Phys 1969;40:485.
[9] Levine E, Kichter J. Proc 22nd IEEE IRPS 1984. p. 242.
[10] Besser PR, Madden MC, Flinn PA. J Appl Phys 1992;72:3792.
[11] Kraft O, Bader S, Sanchez Jr. JE, Arzt E. Mat Res Soc Symp Proc 1993;308:199.
[12] Marieb T, Bravman JC, Flinn P, Madden M. Mat Res Soc Symp Proc 1994;338:409.
[13] Bobbio A, Saracco O. Microelectron Reliab 1975;14:431.
[14] Jones BK. Mat Res Soc Symp Proc 1995;391:489.
[15] Scorzoni A, De Munari I, Stulens H, D'Haeger V. Mat Res Soc Symp Proc 1995;391:513.
[16] Kraayeveld JR, Verbruggen AH, Willemsen AW, Radelaar S. Appl Phys Lett 1995;67:1226.
[17] D'Haeger V, De Ceuninck W, De Schepper L, Stals LM. Mat Res Soc Symp Proc 1996;428:133.
[18] Wen Q, Clarke DR. Mat Res Soc Symp Proc 1996;428:141.
[19] Shingubara S, Kaneko H, Saitoh M. J Appl Phys 1991;69:207.
[20] Li Z, Bauer CL, Mahajan S, Milnes AG. J Appl Phys 1992;72:1821.
[21] Miner B, Sriram TS, Pelillo A, Bill SA. Mat Res Soc Symp Proc 1997;473:351.
[22] Madden MC, Abratowski EV, Marieb TN, Flinn PA. Mat Res Soc Symp Proc 1992;265:33.
[23] Flinn PA, Lee S, Doan J, Marieb TN, Bravman JC, Madden M. AIP Conf Proc 1997;418:250.
[24] Doan J, Bravman JC, Flinn PA, Marieb TN. AIP Conf Proc 1999;491:15.
[25] Kraft O, Arzt E. Appl Phys Lett 1995;66:2063.
[26] Doan JC, Bravman JC, Flinn PA, Marieb TN. Mat Res Soc Symp Proc 1999;563:103.
[27] Flinn PA. Mater Res Bull 1995;20:70.
[28] Gleixner RJ, Clemens BM, Nix WD. J Mater Res 1997;12:2081.
[29] Marieb TN. PhD Thesis, Stanford University, 1994.
[30] Jones BK, Guo J, Xu Y, Trefan G. Mat Res Soc Symp Proc 1998;516:9.
[31] De Ceuninck WA, D'Haeger V, Van Olmen J, Witvrouw A, Maex K, De Schepper L, De Pauw P, Pergoot A. Microelectron Reliab 1998;38:87.
[32] Madelung O, editor. Numerical data functional relationships in science technology. vol. 15. Springer: Berlin, 1996.
[33] Madelung O, editor. Numerical data functional relationships in science technology. vol. 5. Springer: Berlin 1996.
[34] Sanchez Jr. JE, Pham V. Mat Res Soc Symp Proc 1994;338:459.
[35] Verbruggen AH, Van den Homberg MJC, Jacobs LC, Kalkman AJ, Kraayeveld JR, Radelaar S. Mat Res Soc Symp Proc 1997;473:255.
[36] Reilly CJ, Sanchez Jr. JE. J Appl Phys 1999;85:1943.
[37] Niehof J, de Graaff HC, Verwey JF. Mat Res Soc Symp Proc 1993;309:295.
[38] Mouthaan TJ, Petrescu V. Microelectron Reliab 1998; 38:99.
[39] Brown DD, Sanchez Jr. JE, Korhonen MA, Li CY. Appl Phys Lett 1995;67:439.
[40] Simmons RO, Balluffi RW. Phys Rev 1960;117:62.
[41] King HW. J Mat Sci 1966;1:79.
[42] Nakamichi I. J Sci Hiroshima Univ A 1990;54:49.
[43] Shih WC, Greer AL. J Appl Phys 1998;84:2551.
[44] Ainslie NG, d'Heurle FM, Wells OC. Appl Phys Lett 1972;20:173.
[45] Blech IA. J. Appl Phys 1976;47:1203.
[46] Lee S. PhD Thesis, Stanford University, 1999.
[47] Doan JC, Lee S-H, Bravman JC, Flinn PA, Marieb TN. Appl Phys Lett 1999;75:633.